Journal of Cleaner Production 205 (2018) 1127–1138

Contents lists available at ScienceDirect

Journal of Cleaner Production

journal homepage: www.elsevier.com/locate/jclepro

A comparative study on co-pyrolysis of lignocellulosic biomass with polyethylene terephthalate, polystyrene, and polyvinyl chloride: Synergistic effects and product characteristics

Gamzenur Özsin [a, *], Ayşe Eren Pütün [b]

[a] Bilecik Şeyh Edebali University, Department of Chemical Engineering, Faculty of Engineering, Bilecik, 11210, Turkey
[b] Anadolu University, Department of Chemical Engineering, Faculty of Engineering, Eskişehir, 26555, Turkey

ARTICLE INFO

Article history:
Received 2 January 2018
Received in revised form
12 September 2018
Accepted 15 September 2018
Available online 20 September 2018

Keywords:
Biomass
Polyethylene terephthalate
Polystyrene
Polyvinyl chloride
Pyrolysis

ABSTRACT

Co-pyrolysis of waste biomass and plastics was investigated to find out whether the quality of pyrolysis products was improved. For the sake of yield and compositional comparison, three polymers (polyethylene terephthalate, polystyrene, and polyvinyl chloride) and two biomasses (walnut shells and peach stones) were tested in a fixed bed reactor. The maximum bio-oil yield was obtained at 500 °C as 20.81 wt % for walnut shell and 18.30 wt %, for peach stone pyrolysis, then co-pyrolysis experiments were performed at 500 °C. Based on the experimental findings, blending of polyethylene terephthalate, polystyrene, and polyvinyl chloride into biomass affected product yield substantially. To gain more insight into the effect of polymers, liquid and solid products were analyzed by various analytical techniques. Results showed a significant modification on the chemical structure tars after co-pyrolysis, and tar yield increased up to 49.80 wt%. Meanwhile, modifying the structures and enhancing the quality of the tars and chars seemed possible by co-pyrolysis.

1. Introduction

Disposal of organic wastes is a serious environmental problem of mankind considering accelerated industrialization and population growth. The accumulation of waste and the "throw-away philosophy" result in several environmental problems, health issues and safety hazards, and prevent sustainable development in terms of resource recovery and recycling of waste materials. On the other hand, these wastes have a huge potential in lowering the dependence on fossil fuels and producing energy through waste-to-energy (WTE) processes (Herbert and Krishnan, 2016; Taherzadeh and Karimi, 2008). Such technologies have been a viable waste management strategy in establishing sustainable waste disposal methods, and are capable of delivering clean energy and providing better end products in comparison to other disposal methods (Shen et al., 2016). When availability, and economic and environmental benefits are considered as the most crucial factors for proper selection of materials to be used in WTE technologies, it can be seen that non-edible biomass wastes have received increased attention in recent years (Dewangan et al., 2016; Ning et al., 2013). There are many different technologies that are being applied in biomass utilization, including biological, physical and thermochemical conversion. Transformation of the wastes into bioenergy can be efficiently achieved applying thermochemical methods such as combustion, pyrolysis and gasification (Alvarez et al., 2014; Kajaste, 2014). As an effective and promising thermochemical conversion technology, pyrolysis offers several advantages in energy production since it is flexible due to convenient manipulation of process parameters to optimize the product yield based on preferences.

Through pyrolysis process, long-chain polymer molecules are thermally degraded into smaller, less complex molecules by being heated in the absence of oxygen (Sharuddin et al., 2016; Strezov et al., 2008). Pyrolytic oil can be used in boilers and diesel engines for power generation while it may also be used to obtain valuable and useful chemicals, such as flavoring and resins (Bhattacharjee and Biswas, 2017; Guo et al., 2010; Van Putten et al., 2013). The solid product of pyrolysis, char, can either be directly used as fuel since it has a high calorific value or it can be used as feedstock to prepare carbonaceous products such as activated

* Corresponding author.
E-mail addresses: gozsin@anadolu.edu.tr, trgamzenur.ozsin@bilecik.edu.tr (G. Özsin).

https://doi.org/10.1016/j.jclepro.2018.09.134
0959-6526/

carbon. Other potential benefits of char are nitrate leaching, adsorption of inorganic and organic contaminants and reduction of trace-gas emissions from soil and atmosphere (Chen, D. et al., 2016; Lu et al., 2012; Zhao, B. et al., 2018). On the other hand, the gas product can be considered as a mixture composed of carbon oxides, light hydrocarbons, and hydrogen which can be utilized as gas fuel (Chen et al., 2003; Solar et al., 2016). The production of synthetic fuel and value-added intermediates from biomass seems attractive considering renewable nature of biomass (Dorado et al., 2015; Hasan et al., 2017). Still, most of the studies about pyrolysis are mainly focused on how to increase the yield of pyrolytic oil that are produced from lignocellulosic biomass and enhance its properties. The major challenges in converting lignocellulosic biomass to "drop-in" liquid fuels are related to the feedstock properties (Perkins et al., 2018). This is due to several oxygenated products, such as sugars, aldehydes, ketones, acids, and phenols which can be formed during pyrolysis of biomass. Presence of such compounds both lowers the calorific value of bio-oil, causes corrosiveness and instability and hence liquid product of biomass pyrolysis, bio-tar, requires additional separation steps (Chen et al., 2014; Nigam and Singh, 2011; Ro et al., 2017). Therefore, current studies focus on catalytic pyrolysis, hydro-pyrolysis, hydrothermal treatment or co-pyrolysis techniques in order to improve the quality of bio-oil.

Recently, positive effects of plastic blending in biomass have been reported in the literature since plastics can effectively balance the C, H, and O content of the feedstock and eliminate disposal problems of plastics (Chen et al., 2017; Kumagai et al., 2016; Soganciogl u et al., 2017). Lignocellulosic biomass sources are hydrogen deficient, whose H/C ratio usually vary between 0 and 0.3, therefore when they are pyrolyzed, yields of petrochemicals are relatively low. On the other hand, plastic wastes mainly consist of polyolefin, with a higher H/C value than biomass sources. Hence, carbon and hydrogen will be exchanged during the co-pyrolysis reaction, and increase the quality of petrochemicals with co-feeding of plastics with biomass (Chattopadhyay et al., 2016). To put it in other words, polymer blending to biomass creates more free radicals and may suppress formation of long-chain hydrocarbon compounds (Shadangi and Mohanty, 2015). This synergistic effect among plastic-derived olefins and lignin, cellulose, and hemicellulose-derived fragments would lead to a strong improvement on the properties of bio-oils (Chen, W. et al., 2016; Zhao, Y. et al., 2018). Another benefit of co-pyrolysis can be stated as raw material sustainability since using waste mixtures or different feedstock types can help resolve issues related to the limited supply of some feedstock types. Furthermore, it is the least capital intensive process with low operating costs (Melendi-Espina et al., 2015; Oyedun et al., 2014).

In the literature, numerous studies are focusing on the co-pyrolysis of plastics and biomass, in order to investigate product yields and distributions together with product characteristics (Bernardo et al., 2009; Paradela et al., 2009; Sajdak, 2017). Results showed that, positive or negative synergy depend on the type and contact of components, pyrolysis duration, temperature and heating rate, removal or equilibrium of volatiles formed, and addition of solvents, catalysts, and hydrogen-donors. Among these factors, the types of blending feedstock are a major factor that can significantly influence the synergistic effects; thus, synergistic effects on co-pyrolysis can be complicatedly varied (Abnisa and Daud, 2014; Sajdak, 2017). For instance, blending polymers such as polyethylene, polypropylene, polystyrene, polyurethane to specific biomass samples is generally known to increase liquid product yield (Dewangan et al., 2016; Suriapparao et al., 2018; Chattopadhyay et al., 2016) According to the previous researches polyvinyl chloride results in increase in solid product yield (Ephraim et al., 2018; Lu et al., 2018). However, distinctive properties of each biomass species make impossible to reach a general consensus on precise polymer-biomass interactions during co-pyrolysis.

In this study, walnut shells (WS) and peach stones (PST) were selected as biomass species since they are popular plantations and grown in many countries worldwide. About 10 million hectares of land is used for the cultivation of walnut and its annual production is approximately 3.5 million metric tons. On the other hand, an area of 1.5 million hectares is harvested to produce approximately 23 million tons of peach stones throughout the world (FAO, 2017). Hence, a considerable amount of non-edible wastes is discarded during the processing of these fruits. To the best of our knowledge, co-pyrolysis of walnut shells and peach stones with PET (polyethylene terephthalate), PS (polystyrene), and PVC (polyvinyl chloride) has not been reported in the literature yet. These synthetic polymeric wastes selected due to the considerable amount of usage and hence waste generation in the industrial and daily life. PET and PS include aromatic rings in their repeating units which can be produced by the polymerization of ethylene glycol with terephthalic acid and styrene, respectively. On the other hand, PVC is one of the most-widely produced polymer through polymerization of vinyl chloride monomer. Therefore, the aim of this study is to investigate the effect of biomass and different polymer characteristics during co-pyrolysis to evaluate the potentials of the co-pyrolysis products for recovery of chemicals. For this purpose, effects of polymer blending on liquid and solid product characteristics were analyzed and discussed in detail.

2. Methods

2.1. Preparation and characterization of raw materials

In this study, two biomass samples including walnut shell (WS) and peach stones (PST) were used for investigation. Waste PET, PS, and PVC samples were obtained from the post-consumer polymer waste collection establishment in Turkey. After grinding, all samples were sieved to obtain a uniform particle size between 1 and 1.25 mm to be used in a fixed-bed reactor. On the other hand, a particle size between 112 μm and 224 μm was used for TGA. The blends were prepared by mixing the samples at a definite ratio of 50 wt %. Prior to pyrolysis and co-pyrolysis experiments, TGA was performed for the raw materials and blends in a Setreram-Labsys Evo thermobalance. In each analysis, approximately 10 mg of sample was put uniformly in an Al_2O_3 ceramic crucible and heated from 25 °C to 1000 °C at a constant rate of 10 °C min^{-1} in a nitrogen atmosphere with a flow rate of 20 ml min^{-1}.

2.2. Pyrolysis experiments

The pyrolysis experiments were conducted in a fixed-bed reactor system, which is illustrated in Fig. 1. In each trial, 10 g of raw material (or blend with a 50 wt %) was put inside the reactor, and then the reactor was closed tightly with an input pipe for inert gas connection and output pipe was connected to the liquid product collecting traps. Before each run, nitrogen was purged through the reactor for 10 min to ensure an inert atmosphere.

The pyrolysis experiments were performed to study the effect of pyrolysis temperature in the range 400–700 °C and then co-pyrolysis experiments were carried out at 500 °C. A thermocouple was installed near the center of the sample chamber to enable measurement of the temperature and the desired temperature was adjusted using an automatic PID controller. The volatile products left the reactor together with the inert gas and condensable gases were converted to liquid as the volatile products passed through the traps containing salty-ice. The liquid products were recovered

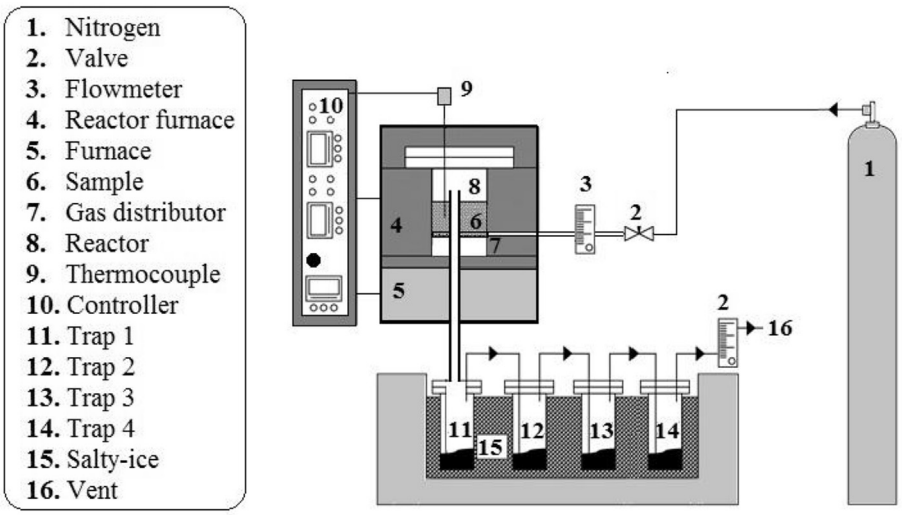

Fig. 1. Schematic diagram of the reactor.

by washing the traps and the connection lines with dichloromethane (CH_2Cl_2). Water and pyrolytic oil dissolved in dichloromethane were then separated by a separation funnel, and pyrolytic oil was passed over anhydrous sodium sulfate in order to remove all of the remaining aqueous phases. Afterwards, dichloromethane that was used in the extraction was removed by a rotary evaporator, and liquid products were obtained. After the reaction was completed, char was collected from the reactor, and the gas yield was calculated by taking the difference from mass balance. All experiments were repeated in triplicates and calculated yields were reported as dry-ash free basis.

2.3. Characterization of the products

In order to characterize the products obtained from the pyrolysis and co-pyrolysis experiments, liquid and solid products were analyzed by various techniques. For the characterization of liquid products, GC-MS, ^{1}H-NMR, and elemental analysis were used. On the other hand, SEM and elemental analysis were used in the characterization studies of solid products. GC-MS analyses of the pyrolytic oils were carried out using a Hewlett-Packard HP 7890 gas chromatograph coupled to an HP 5975 quadrupole detector. Prior to the GC-MS analyses, the oils were dissolved in dichloromethane. The gas chromatograph was equipped with a 30 m × 0.25 mm capillary column coated with a 0.25 μm thick film of 5% phenylmethylpolysiloxane (HP-5). The carrier gas was helium with a constant flow rate of 1.2 ml min^{-1}. The oven was programmed to hold at 40 °C for 5 min, then ramped up at a rate of 2 °C min^{-1} to 290 °C and held for 20 min. Chromatographic peaks were identified by mass spectral data library and from their retention times. The percentages of the peaks were calculated from the TIC (total ion chromatogram) peak area. NMR analyses were performed using a Bruker Ultrashield 500. For this purpose, the samples were diluted in tetramethylsilane (TMS) containing deuterated chloroform ($CDCl_3$). Elemental analyses of the liquid and solid products were performed by a CHN–S Analyzer (LECO CHN628) in order to determine elemental compositions together with calorific values of the products. Surface morphologies of the chars were explored using scanning electron microscopy (SEM). For this purpose, an SEM (Carl Zeiss Supra 50 VP) was used to obtain high-resolution secondary electron images and to investigate surface morphologies.

3. Results

3.1. Analysis of raw materials

Prior to the pyrolysis and co-pyrolysis experiments, which were conducted in a fixed-bed reactor, characteristics of the raw materials were determined and the results are summarized in Tables 1–3. When the proximate analysis results of the biomass samples were evaluated, it was found that the content of volatiles and moisture in WS are slightly higher (76.45 and 6.98 wt %). From a biochemical composition perspective, high lignin contents of both samples were noticeable. The highest lignin content was found in PST as 39.26 wt %, while it was 36.89 wt % in the WS structure. When the ash composition was investigated, lower ash content than volatiles shows that the biomass materials are suitable to use in pyrolysis since higher ash content of biomass may cause slagging, corrosion and fouling (Trubetskaya et al., 2015). When the ash composition was investigated in detail, K_2O and CaO contents were found higher than other inorganic compounds. The oxides of alkali/alkaline earth metals present in ash are known to catalyze secondary reactions thereby reducing the activation energy during pyrolysis and may affect product yields by decreasing yield of tars and favoring formation of char, water and gaseous products (Johansson et al., 2018; Mallick et al., 2018).

In order to determine the structural changes in the solid matrix during pyrolysis and co-pyrolysis, SEM images of raw biomass samples were also obtained and are given in S1. Accordingly,

Table 1
Proximate and component analyses of biomass samples.

	WS	PST
Proximate analysis (%)		
Moisture (ASTM E871-82, ASTM E870-82)	6.98	6.88
Ash (ASTM D1102-84, ASTM E870-82)	0.58	0.86
Volatiles (ASTM E872-82, ASTM E870-82)	76.45	72.42
Fixed carbon[a]	15.99	19.84
Component analysis (%)		
Hemicellulose (ASTM E–1757, ASTM D-1695)	26.20	25.10
Lignin (ASTM E–1757, ASTM D1106-96)	36.89	39.26
Extractives (ASTM E–1757, ASTM D1107-96)	4.14	5.28
Cellulose[a]	32.19	29.50

[a] From difference.

Table 2
Mineralogical analyses of biomass samples.

Ash	WS	PST
Na_2O	1.830	1.604
MgO	4.240	11.872
SiO_2	1.092	2.322
Al_2O_3	–	0.513
P_2O_5	4.886	13.562
CaO	39.254	18.757
MnO	0.084	0.301
Fe_2O_3	0.759	7.020
K_2O	43.681	40.516
SO_3	3.512	3.062
CuO	–	0.274
ZnO	–	0.114
SrO	0.172	–
BaO	0.364	–
Cl	0.126	–
Cr_2O_3	–	0.083

Table 3
Elemental analysis of the samples.

	WS	PST	PET	PS	PVC
C (%)	47.52	49.28	61.62	90.34	47.97
H (%)	6.71	6.65	4.73	9.06	5.28
N (%)	0.21	0.34	0.26	0.29	0.38
O[a] (%)	45.56	43.73	33.38	0.31	–
H/C	1.683	1.609	0.914	1.196	1.311
O/C	0.720	0.666	0.407	0.003	–
Calorific value (MJ/kg) [b]	17.536	18.379	21.639	43.576	–

[a] From difference.
[b] From Dulong's equation.

biomass samples had a non-porous particle profile with a smooth heterogeneous surface.

3.2. Pyrolytic and co-pyrolytic characteristics of samples in TGA

TG and dTG curves reveal weight loss as a function of temperature arising from phase transitions during pyrolysis reactions. Hence, TG and dTG curves of the samples and their blends are given in Fig. 2. Thermal decomposition of WS and PST mainly consisted of three weight loss stages: loss of moisture bound (from ambient temperature up to approximately 175 °C), active pyrolysis in the appropriate temperature range (approximately between 180 °C and 480 °C), and passive pyrolysis due to secondary decomposition at high temperatures over 700 °C. At the end of the active pyrolysis zone, WS lost 61.36 wt % of its initial weight while PST lost 59.78 wt %.

When it comes to degradation of polymers used in the experiments, breaking down of virgin PS and PET seems to occur in a single step, while PVC degradation takes place in multiple steps. It is known that PVC degradation has two characteristic distinct stages as dehydrochlorination relatively lower temperatures followed by cracking and decomposition of the dehydrochlorinated PVC at higher temperatures (Yu et al., 2016). For PVC, the decomposition temperature range was recorded between 235 °C and 534 °C and 13.58% of the initial weight remained after decomposition. On the other hand, residues of approximately 6.44 and 18.86 wt % of the sample weight remained after thermal decomposition of PS and PET, respectively. The peak temperature of PET with a maximum mass loss rate (431 °C) was very close to that of PS (436 °C), while the peak temperature of PVC (286 °C) was the lowest. The structural properties of the biomass/polymer blends were affected by the constituents, and these results are also indicated in the TG and dTG curves. Blending PET, PS, and PVC seemed to delay the initiation point of pyrolysis reactions, and both type of the biomass and type of the polymer affected the characteristic temperatures.

3.3. Pyrolysis and co-pyrolysis product yields

Fig. 3 shows the product yields obtained during the pyrolysis of WS and PST at temperatures from 400 °C to 700 °C. The maximum tar yields of 20.81 (±0.82) and 18.30 (±1.01) wt. % (dry, ash-free basis) were obtained at 500 °C for WS and PST, respectively. Further increase in pyrolysis temperature, resulted in a decrease in tar yield. This is primarily attributed to the secondary cracking of the bio-oils at higher temperatures. The yield of non-condensable gases increased with increasing pyrolysis temperature for both of the biomass samples as the pyrolysis temperature increased from 400 °C to 700 °C. In contrast, the char yields decreased with increasing pyrolysis temperature. Char yields were determined as 30.58 (±0.18) for WS and 33.56 (±0.36) wt. % for PST at 500 °C. Since PST has higher lignin content than WS, char formation was higher in the case of PST pyrolysis.

With respect to co-pyrolysis with PET, PS, and PVC, product yields are presented in Fig. 4 together with the product yields of polymer pyrolysis. During pyrolysis of PET, PS, and PVC, almost all of the material decomposed as mainly liquid and gas products, and a negligible amount of char was observed as soot formation in the reactor. Several authors also stated previously that char fraction of plastic materials is only a minority of total weight, which can be neglected (Encinar and González, 2008). In the case of PET pyrolysis, 76.20 wt% of the material was converted into gaseous products while gas yield of PVC pyrolysis was 83.88 wt %. In the case of PS pyrolysis, the observation was different, in that tar was higher than gaseous products as its yield was 68.80 wt %. The highest gas product yield occurring in PVC pyrolysis was mainly attributed to the chloride ion, which eases decomposition due to its high electronegativity.

In order to evaluate synergetic effects, theoretical yields were calculated based on the weighted average of individual pyrolysis yields, and a comparison between experimental and theoretical yields was done. The theoretical tar yields of WS/PVC and PST/PVC co-pyrolysis were calculated as 18.46 and 17.21 wt %, respectively. On the other hand, the experimental tar yields of WS/PVC and PST/PVC were 17.60 and 14.70 wt %. This indicates an antagonistic effect of PVC on liquid product yields during co-pyrolysis. However, PET and PS caused a synergetic effect to enhance liquid product yield during the co-pyrolysis. Experimental liquid product yield increased to 28.90 and 23.45 wt % for WS/PET and PST/PET, respectively, while their theoretical values were 22.30 and 21.05 wt %. As expected, the highest co-pyrolytic tar yield was obtained in the case of blending PS. For WS/PS and PST/PS, the experimental tar yields (44.81 and 49.8 wt%) were higher than that of the theoretical yields (43.71 and 43.55 wt %). These phenomena meant that interactions between PET and PS and lignocellulosic fragments might exert a positive effect on condensable liquid products. These synergetic effects in co-pyrolysis could be attributed to radical interaction during co-pyrolysis. Synthetic polymers act as hydrogen donors in thermal co-processing with biomass because of their high hydrogen content relative to biomass. It may be stated that the tar yields were comparable, and promising for the production of fuel and chemicals. For all biomass/polymer pairs, the theoretical gas products yields were found to be higher than the experimental gas yields. This is due to secondary reactions of radicals, which cause condensation reactions of non-condensable fragments. In terms of char yield, co-processing polymers with biomass samples decreased char yields substantially. The highest co-pyrolysis char

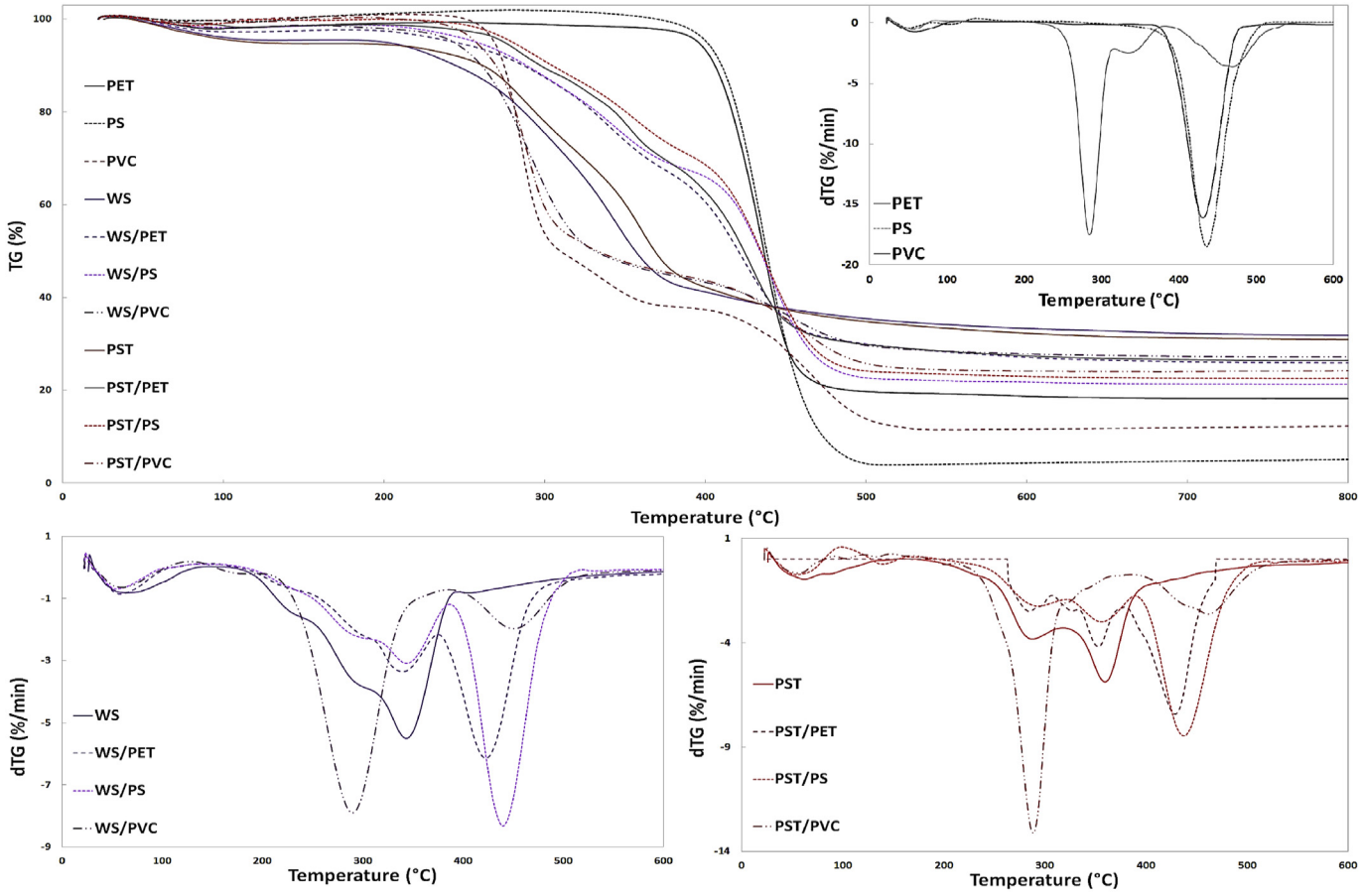

Fig. 2. TG and dTG curves of the samples and the blends.

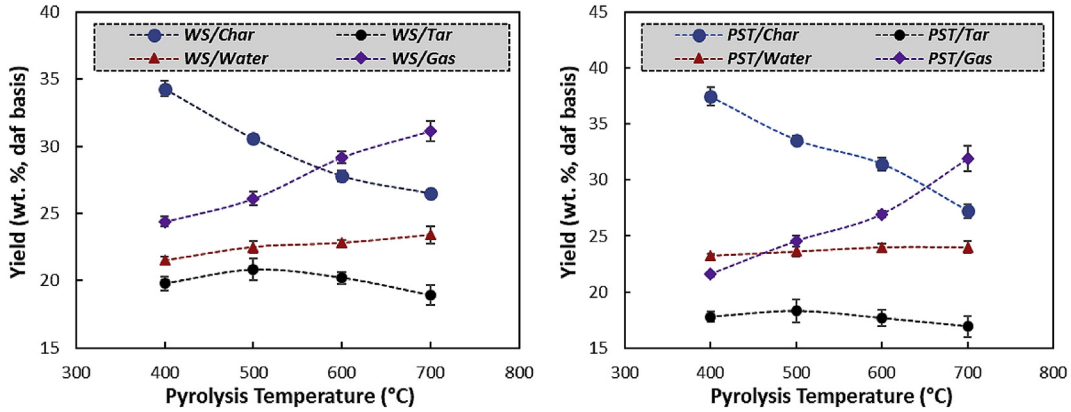

Fig. 3. Effect of pyrolysis temperature on product yields of biomass pyrolysis.

yields were obtained in the case of PET blending (25.90 and 28.50 wt % for WS/PET and PST/PET) while the lowest yields were obtained in co-pyrolysis with PVC (19.98 and 20.30 wt % for WS/PVC and PST/PVC).

3.4. Characterization of liquid products

3.4.1. ^{1}H-NMR analysis

^{1}H-NMR analysis of the tar samples was performed to understand the ratios of protons in chemical environments. Based on the proton type, four different groups of compounds can be identified in the structure of pyrolytic and co-pyrolytic tars as carbonyl (10.5–9.0 ppm), aromatic (9.0–6.0 ppm), oxygenated phenols (6.0–4.0 ppm), and aliphatic compounds (4.0–0.5 ppm). Integration results are presented in Table 4 for quantifying the proton ratios of the tars and the spectrums are given in S2. The aromaticity of the pyrolytic and co-pyrolytic tars was evaluated in particular since there is a growing interest to produce aromatic hydrocarbons by pyrolysis process due to their widespread application in chemical industry. Industrial applications of aromatics have been unearthed for octane enhancement or as raw materials for the production of value-added solvents, plastics and synthetic fibers

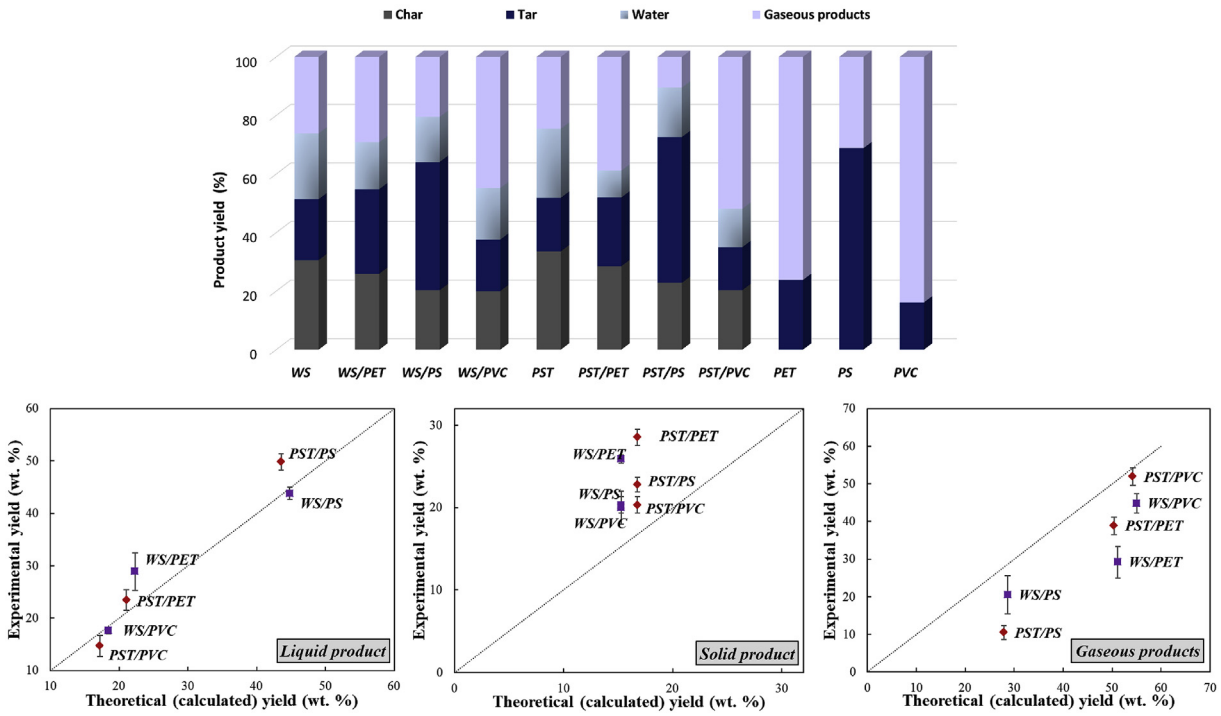

Fig. 4. Pyrolysis and co-pyrolysis product yields (Pyrolysis temperature = 500 °C).

Table 4
^{1}H-NMR results of the pyrolytic and co-pyrolytic tars.

Chemical shift (ppm)	Main assignments of type of protons	Functionality	WS (%)	WS/PET (%)	WS/PS (%)	WS/PVC (%)	PST (%)	PST/PET (%)	PST/PS (%)	PST/PVC (%)
10.5–9.0	R-(H-)C=O, –CHO, –COOH, downfield	Carboxylic acid and aldehyde protons	1.82	1.50	0.20	0.00	2.46	1.04	0.79	0.00
9.0–6.8	ArH, HC=C-(conjugated)	Aromatic protons including guaiacyl units	7.46	52.91	52.30	33.34	11.20	38.20	54.50	31.41
6.8–6.0	ArH, HC=C-(non-conjugated)	Aromatic protons including syringyl units, aromatic and non-conjugated alkenes	13.52	3.40	5.50	0.19	12.55	4.82	1.87	0.49
6.0–4.0	$-CH_n$-O–,$-CH_n$-OH, =CHO, ArH, ArOH, HC=C (non-conjugated), Ar–CH_2–O-aliphatic OH	Vinyl, carbohydrates, methoxys, nonconjugated alkenes, aromatic ethers, non-conjugated olefinic proton	6.91	7.92	13.38	0.00	8.36	7.21	10.08	0.55
4.0–2.0	CH_3O-,$-CH_2O$-,–CHO–,α- to oxygen, ring-join methylene (Ar–CH_2–Ar) H–C–OH, H-COR, RCOO-C–H $CH_3C(=O)$-, CH_3–Ar,$-CH_2Ar$, $CH_α$-to aromatic,$-CH_3$,$-CH_2$, $CH_2C=O$, CC–H, Ar–C–H, H–C-COOR, H–C–COOH, H–C–C=O, $C=CCH_3$	α-Hydrogen atoms of branched chain of aromatic ring carbons, methoxy, and aliphatic OH	60.26	28.49	15.11	40.43	51.50	35.44	27.88	42.41
2.0–1.0	$-CH_2-$, aliphatic OH, CH_2 and CH attached to naphthenes, and $CH_β$ to an aromatic ring (naphthenic), $-CH_3$, $-CH_2$, $-CH_β$, β-CH_3,$-CH_2$, and $CH_γ$ or further to aromatic ring	Aromatic β-hydrogen atoms and methylene hydrogen atoms in alkanes	10.03	5.77	11.17	19.31	12.15	11.37	4.48	18.31
1.0–0.5	γ-CH_3 or further from an aromatic ring and paraffinic CH_3	Alkanes, aliphatics, aromatic γ-hydrogen atoms and methyl hydrogen atoms in alkanes	0.00	0.00	2.34	6.72	1.78	1.91	0.39	6.82
	Aromaticity (%)		22.79	57.44	57.99	33.53	23.75	44.06	56.37	31.90

(Lee et al., 2016; Kelkar et al., 2015) Therefore, several pyrolysis studies have been aimed to increase selectivity towards to aromatics by applying co-pyrolysis processes or catalytic pyrolysis (Chang et al., 2018; Sun et al., 2016; Zhang et al., 2018). According to the results, the aromaticity of the tars obtained from co-pyrolysis with PET, PS, and PVC was higher compared to that of the tar obtained by pyrolysis of the biomass alone. The aromaticity of tar produced by pyrolysis of WS was 22.79%, while the aromaticity of PST tar was 23.73%. Furthermore, α-hydrogen atoms of the branched chain of aromatic ring carbons, methoxy, and aliphatic hydroxyl contributed more to the hydrogen functionality of WS and PST tars than other functionalities. This may indicate that main constituents of lignocellulosic structures; lignin, cellulose and hemicellulose, have been thermally cracked to smaller functional groups. Overall, a few oxygenated phenols with negligible carbonyls were found in the structures of the bio-oils of WS and PST. In the case of co-pyrolysis with PET and PS, aromatic protons including guaiacyl units increased substantially, while PVC

blending resulted in an increase in both aromatic protons including guaiacyl units and α-hydrogen atoms of the branched chain of aromatic ring carbons, methoxy and aliphatic hydroxyl. This may be due to the structure of PET and PS that contain aromatic monomers and condensation of polyenes and aromatization during PVC decomposition. It is generally accepted that chlorine radicals that are formed during decomposition of PVC may cause aromatization, cyclization and condensation reactions (Liu et al., 2018).

The region of 9.0–6.0 ppm accounted for 57.44%, 57.99%, 33.53%, 44.06%, 56.37%, and 31.90% of the total area for WS/PET, WS/PS, WS/PVC, PST/PET, PST/PS, and PST/PVC, respectively.

3.4.2. GC-MS analysis

Primary pyrolysis and co-pyrolysis compounds and their relative proportions obtained at a pyrolysis temperature of 500 °C were analyzed by GC-MS. GC-MS analysis provides data at a molecular level, in which mass spectrum gives the structural information of compounds separated by gas chromatogram (Wang et al., 2013). Accordingly, chromatographic peaks were identified by spectral data library and the percentages of the peaks were calculated from the TIC peak area. Table 5 gives the classification and peak-area percentage of samples together with the main peak and its corresponding compound and Fig. 5 shows obtained chromatograms during analysis. Furthermore, comparative lists of identified compounds can be found in Supplementary files (S3 and S4).

When the tars produced by the pyrolysis of biomass alone were analyzed several oxygenated products such as lignin-derived phenolics, acids, alcohols, aldehydes, ketones were found in the structures of WS and PST tar. However, it was seen that the largest constituent class was phenol and its derivatives, which mostly came from the decomposition of lignin. Lignin is a complex aromatic structure and is composed of substituted phenyl propane units, linked by hydroxyl and methoxy groups, and decomposition of this natural polymer causes formation of phenolics (Mei and Liu, 2017). Cracking of the side chains or breaking of the internal ether bonds and C–C bonds of lignin during pyrolysis causes the formation of various free radicals containing a benzene ring; subsequently, various aromatic compounds may be generated. The compounds of lignin pyrolysis are predominantly phenolic compounds, which are more complex and mostly contained methoxy-substituents, benzenediols, and polysubstituted phenols and formed by the fracture of main chain and complex reactions of alkyl side chains such as dehydration, decarbonylation, decarboxylation, demethylation and alkylation (Zheng et al., 2018). However, due to the significant complexity of the decomposition reactions, the various characteristics and the relative distribution of the aromatic derivatives attained through lignin pyrolysis would be based on different factors, such as the type of feedstock and its preparation methods together with and reaction conditions (Jung et al., 2015). WS bio-oil had more phenol and derivatives (58.54%) than that of PST (49.17%), and the main phenolic compounds observed in the structure of bio-oils were alkyl phenols (especially o,m,p-cresol) and methoxy phenols. The major phenols were 4-phenol, 2,6-dimethoxy- (18.30%) for WS and phenol, 2-methoxy-4-methyl- (11.36%) for PST. The compounds in bio-oil mainly consisting of aldehydes, ketones, acids, esters, ethers, furans, alcohols, and hydrocarbons were obtained from the decomposition of cellulose and hemicellulose. On the other hand, PAH's and their derivatives were not identified in the case of biomass pyrolysis.

It is remarkable that the amount of acid and esters were considerably increased during the co-pyrolysis of biomass with PET, while the relative amount of phenolics and ketones decreased. It is well known that pyrolytic oils with such acidic characteristics can create some problems in pyrolysis systems due to corrosion. The percentage of total acids and esters was 65.87% for co-pyrolysis of WS/PET and 63.11% for co-pyrolysis of PST/PET. It has been well established that PET decomposition is initiated by beta scission at the carboxylic group where the ester link is broken to form benzenecarboxylic acid and vinyl benzoate. As temperature keeps increasing the amount of vinyl benzoate formed further decomposes into other aromatic compounds in the wax fraction and lighter compounds in the gas phase (Diaz-Silvarrey et al., 2018). After main pyrolysis stage, nearly half of PET may be decomposed as benzenecarboxylic acid producing carboxylic acid and olefin end groups (Çepelioğullar and Pütün, 2014). This scission may then yield many different gaseous substances (primary products), which further react among themselves (Dimitrov et al., 2013). Accordingly, co-pyrolytic tars of both WS/PET and PST/PET yielded benzenecarboxylic acid in their structures by more than 40%. Formation of PAH's was also observed during the co-pyrolysis of PET.

Regarding the effect of PS during co-pyrolysis with biomass, it can be said that pyrolysis liquid product of WS/PS and PST/PS pyrolysis contained a considerable amount of benzene and its derivatives, with a percentage of 80.78% and 88.46%, respectively. This is because, pyrolysis of PS produces benzene, toluene, and styrene along with other low molecular weight aromatic hydrocarbons. PS pyrolysis is known to produce the monomer, styrene, via end-chain β-scission or unzipping reaction (Suriapparao et al., 2018). The high yields of aromatic compounds are due to thermal degradation of PS, which produces radical chain ends by scission of the main chain

Table 5
Class-wise distribution of compounds in pyrolytic and co-pyrolytic tars using GC-MS (area %).

Main peak	WS (%)	WS/PET (%)	WS/PS (%)	WS/PVC (%)	PST (%)	PST/PET (%)	PST/PS (%)	PST/PVC (%)
	Phenol, 2,6-dimethoxy-	Benzenecarboxylic acid	3-Octen-2-one, 8-phenyl-	Naphthalene	Phenol, 2-methoxy-4-methyl-	Benzenecarboxylic acid	Styrene	Naphthalene, 1-methyl-
Retention time of the main peak (min)	35.40	24.94, 25.64, 36,35	61.54	28.19	25.01	23.99, 25.65, 26.28, 28.85, 29.03	7.47	31.14
Integration result of the main peak (%)	18.30	51.53	18.30	5.78	11.36	42.98	49.22	6.51
Class								
∑Phenol derivatives	58.54	23.88	4.96	2.96	49.17	19.40	3.94	6.17
∑Benzene derivatives	10.63	5.72	80.78	30.04	7.87	10.87	88.46	31.16
∑PAH's and derivatives	–	2.42	4.34	64.40	–	1.90	3.42	59.06
∑Ketones	3.69	2.12	1.49	–	9.05	1.30	0.90	0.28
∑Acids and esters	19.33	65.87	3.67	0.37	12.27	63.11	1.10	1.79
∑Alcohols	5.46	–	2.10	–	10.70	1.16	0.57	0.50
Others[a]	2.35	–	2.65	2.23	10.91	2.25	1.62	1.04

[a] Miscellaneous alkanes, alkenes, alkynes, aldehydes, hetero-compounds and unidentified.

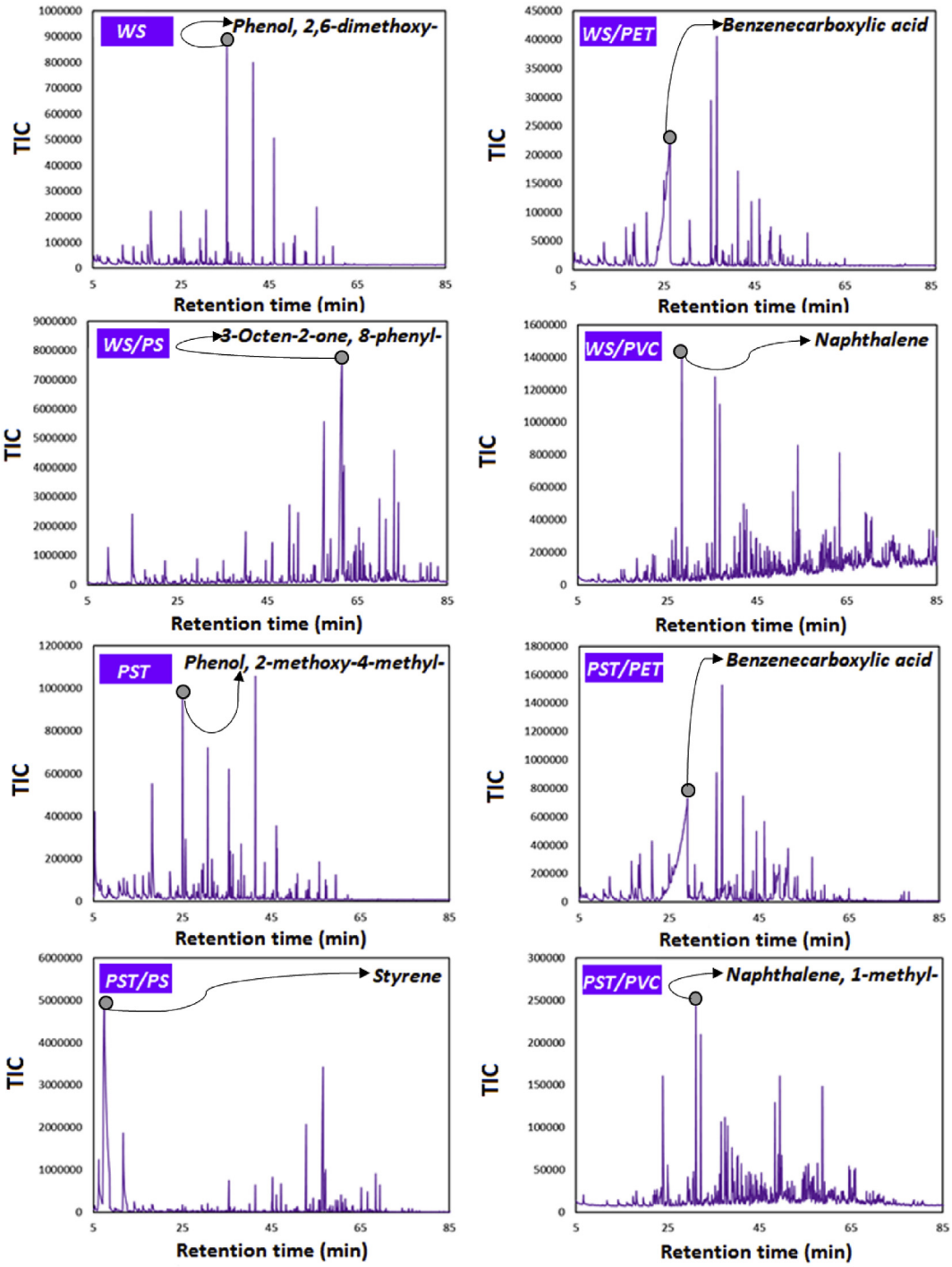

Fig. 5. GC-MS chromatograms of tarry products produced by pyrolysis and co-pyrolysis.

followed by a depolymerization or an intramolecular hydrogen abstraction (back-biting reaction). Monomer molecules are generated mainly by a depolymerization, but oligomers such as dimers and trimers are formed by a back-biting reaction followed by β-scission (Artetxe et al., 2015; Gui et al., 2013; Shadangi and Mohanty, 2015). Hence, the majority of aromatics formed during the co-pyrolysis of WS/PS and PST/PS were believed to be formed through free radicals originating from thermal decomposition of PS.

When the class-wide distribution of co-pyrolytic oils produced by co-pyrolysis of WS/PVC and PST/PVC were investigated, formation of PAH's was noticeable. In the case of WS/PVC co-pyrolysis, the amount of the PAH's and their derivatives was 64.40%, while this amount for PST/PVC was 59.06%. Furthermore, the amount of benzene derivatives was noteworthy as 30.04% for WS/PVC and 31.16% for PST/PVC. Only a small amount of phenol and its derivatives was identified in the tars produced by co-pyrolysis with PVC due to the prominent effect of PVC decomposition, which prompted aromatization reactions and formation of heavier tar components through dechlorination accompanied by inner cyclization; aromatic chain scission and release of two or three

aromatic-ring containing groups prior to the coke formation (Gui et al., 2013). Tang et al. explained the formation of heavier compounds such as PAHs during co-pyrolysis of biomass and PVC due to the HCl release which prompted the evolution of light tar components to heavy components and then caused the formation of higher molecular weight substances (Tang et al., 2018). A similar observation of the work carried out by Zhou et al. concluded that aromatic ringed structures in the PVC tar (which were mainly 1-methylnaphthalene, 2-methylnaphthalene, acenaphthylene, acenaphthene, and benzo [a]anthracene) may be formed directly from chain scission process after dehydrochlorination process of PVC molecules (Zhou et al., 2015). Çepelioğullar and Pütün compared the PVC tar composition with the co-pyrolytic tars of different biomass-PVC pairs and observed considerable amount PAHs and derivatives, which was also found mainly in pure PVC pyrolysis (Çepelioğullar and Pütün, 2014).

3.4.3. Elemental analysis of liquid products

The amount of elemental carbon, hydrogen, and nitrogen present in the products was determined by an elemental analyzer while the oxygen content was calculated by the difference. All of the analysis results are reported after triple measurements and the average elemental composition, together with H/C ratio and calorific value, are given in Table 6. According to the results, the elemental composition of the bio-oil obtained by the pyrolysis of WS was found to be comparable to the composition of PST.

The elemental composition of the liquid product obtained by the pyrolysis of WS was 63.10 wt % carbon, while PST pyrolysis yielded a liquid product which included 62.00 wt% carbon. The higher heating value of these two biomass samples was estimated by Dulong's equation and found to be approximately 24 MJ/kg. The pyrolytic oils were characterized by a lower oxygen content compared to their precursors. When the analysis results of co-pyrolytic tars were evaluated, it was clearly seen that PET, PS, and PVC blending decreased the oxygen content and H/C ratio, and increased calorific values of the liquid products. Since lower oxygen content makes the liquid product more stable, and higher carbon content is required to enhance the calorific value, the most promising co-pyrolysis oil may be stated as WS/PVC which has H/C and O/C ratios of 1.08 and 0.03, respectively.

3.5. Characterization of solid products

SEM and elemental analysis were used for the characterization of chars. Fig. 6 illustrates SEM micrographs of the chars obtained during pyrolysis and co-pyrolysis. It may be seen that significant morphological variations were present because of the radical interactions of PET, PS, and PVC with WS and PST. According to the micrographs of bio-chars (WS and PST), the structures were more fragmented and porous than the parent biomass samples (S1) because of thermal cracking. It is generally believed that macromolecular structure of biomass changes as a result of depolymerization, vaporization, and cross-linking of the solid matrix, causing aromatic ring rupture, and forming a carbonaceous char while the volatiles are evolving (Asadullah et al., 2010; Vyas et al., 2017). It may be concluded that various residual chars with different surface morphologies can be obtained by addition of different polymers during thermal degradation. In the case of co-pyrolysis with PET, many cavities, wreckages, and interconnected pores were observed in the secondary electron images of WS/PET and PST/PET. On the other hand, PS induced the breaking down of the carbonaceous matrix since the disintegration of the particles was visible in the micrographs of WS/PS and PST/PS. By looking at the surface topography of chars produced by co-pyrolysis with PVC (WS/PVC, PST/PVC), it may be stated that PVC was molten into the lignocellulosic structure and various large pores were strongly formed in the external surface. The effect of PVC is known to be decrease the surface area by blocking pores and make surface morphology more agglomerative and smooth due to softening of PVC (Lu et al., 2018; Xu et al., 2016). On the other hand, chars produced by co-pyrolysis with PET and PS may be utilized in some applications such as adsorption, catalysis or preparation of functional composites or anode materials.

Elemental analysis of the chars is also shown in Table 6 for comparison. The content of carbon in the WS char increased from 76.41 wt % to 84.66 wt % during co-pyrolysis with PET. On the other hand, the oxygen content decreased from 18.71 wt % to 11.03 wt %. The effects of PS and PVC in terms of carbon and oxygen content were found to be less significant in enhancing the quality of the char. Apart from the WS biomass, the best PST co-pyrolysis char was obtained in the case of PVC blending, since PST/PVC char had the highest calorific value of 32.08 MJ/kg. The calorific value of the char varied roughly between 27 and 32 MJ/kg during pyrolysis depending on the type of the biomass-polymer pairs. Considering that the calorific values of WS and PS were 17.536 and 18.379, it is noteworthy that all the chars were acceptable for use as a solid fuel. Furthermore, the chars produced by co-pyrolysis with PET, PS, and PVC can withstand longer storage times during storage and provide

Table 6
Elemental analysis of liquid and solid products.

	WS	WS/PET	WS/PS	WS/PVC	PST	PST/PET	PST/PS	PST/PVC
Liquid products								
C (%)	63.10	64.70	72.52	87.96	62.00	65.01	70.59	85.47
H (%)	6.91	5.92	7.31	7.94	6.39	5.56	7.21	7.63
N (%)	0.57	0.18	0.42	0.20	1.01	0.43	0.67	0.20
O (%)[a]	29.42	29.20	19.75	3.90	30.60	29.00	21.53	6.70
H/C	1.30	1.09	1.20	1.08	1.23	1.02	1.22	1.06
O/C	0.35	0.34	0.20	0.03	0.37	0.34	0.23	0.06
Calorific value (MJ/kg)[b]	24.38	25.14	31.50	40.52	24.67	24.78	30.39	38.71
Solid products								
C (%)	76.41	84.66	76.32	83.63	81.55	85.33	70.56	85.46
H (%)	4.44	3.70	3.39	3.59	3.67	3.78	3.22	3.51
N (%)	0.44	0.61	0.48	0.54	0.57	0.53	0.55	0.51
O (%)[a]	18.71	11.03	19.81	12.24	14.21	10.36	25.67	10.52
H/C	0.69	0.52	0.53	0.51	0.54	0.53	0.54	0.49
O/C	0.18	0.09	0.19	0.11	0.13	0.09	0.27	0.09
Calorific value (MJ/kg)[b]	28.87	31.97	27.14	31.26	30.31	32.44	23.88	32.08

[a] From difference.
[b] From Dulong's equation.

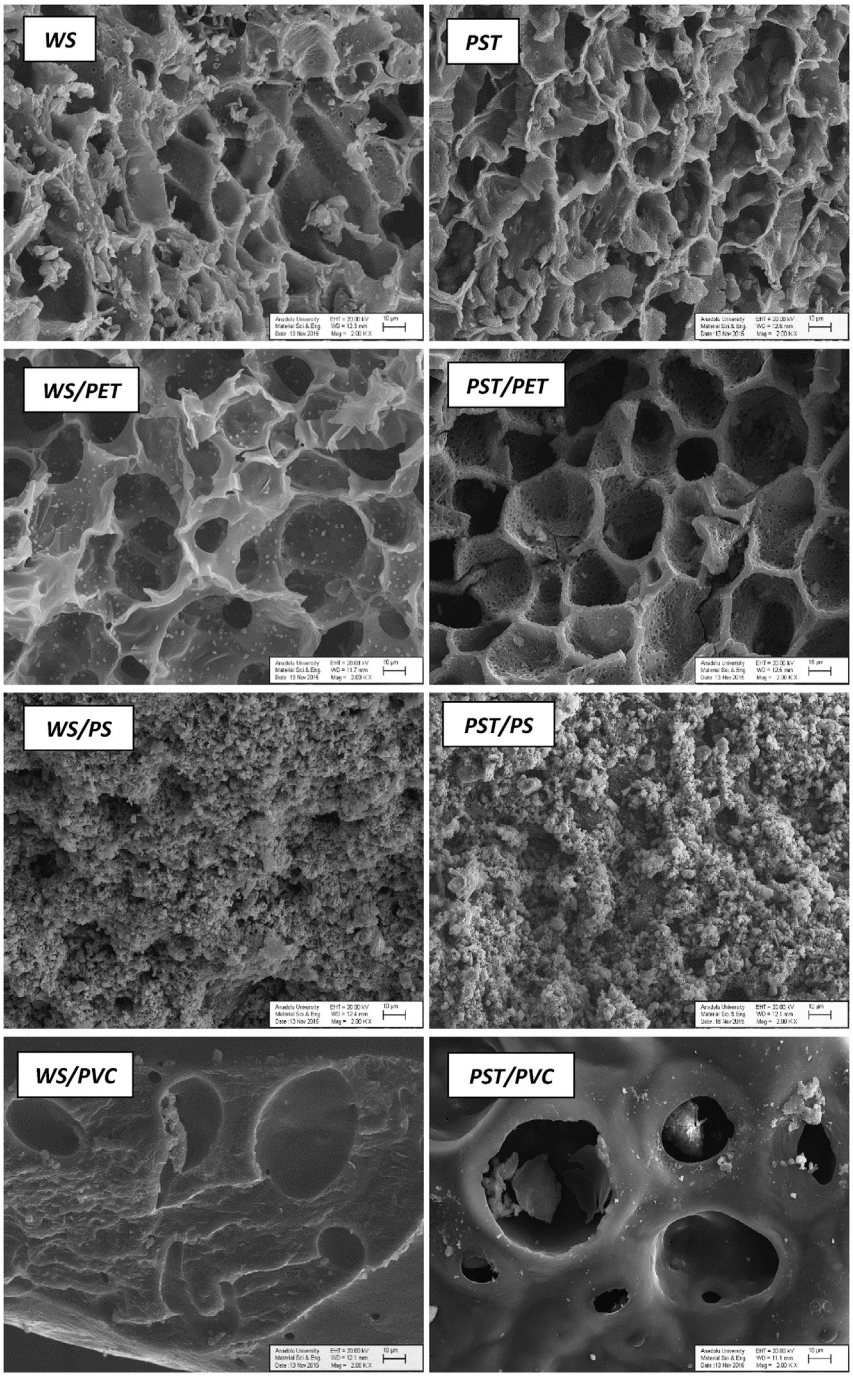

Fig. 6. SEM micrographs of chars.

lower energy loss, gas and steam emissions during combustion due to their lower H/C and O/C ratios caused by aromatization (Liu et al., 2013; Mafu et al., 2017; Wang et al., 2017).

4. Conclusions

The aim of this study was to investigate the effects of polymeric wastes in co-pyrolysis on product yield and distribution, along with the chemical composition of the products. Regarding the effects of PET, PS, and PVC on the yields of products, it may be concluded that synergetic effects and product characteristics highly depended on polymer-biomass pairs. In terms of liquid product yields, co-pyrolysis with PET and PS caused a synergetic effect to increase yields substantially. On the other hand, an antagonistic effect of PVC on liquid product yields during co-pyrolysis were observed. Furthermore, all of the examined polymers decreased the oxygenated compounds and increased calorific values of the liquid products which may be an indication of co-pyrolytic tars can be further used as chemical feed stock and fuel substitute. Also, PET, PS and PVC blending to biomass caused to increase aromaticity of the tars substantially and the detailed composition of the co-pyrolytic tars were determined by GC-MS analysis. According to the results, modifying and tailoring the structures and enhancing quality of the products for the target use seemed possible by using

different plastic wastes through co-pyrolysis. Consequently, co-pyrolysis can be an environmentally friendly technique in waste treatment for transformation and recycling of commingled biomass and polymeric wastes into valuable products.

Acknowledgements

The authors gratefully acknowledge the financial support for this research by the TÜBİTAK through BİDEB 2214-A fund.

Appendix A. Supplementary data

Supplementary data to this article can be found online at https://doi.org/10.1016/j.jclepro.2018.09.134.

References

Abnisa, F., Daud, W.M.A.W., 2014. A review on co-pyrolysis of biomass: an optional technique to obtain a high-grade pyrolysis oil. Energy Convers. Manag. 87, 71–85.
Alvarez, J., Kumagai, S., Wu, C., Yoshioka, T., Bilbao, J., Olazar, M., Williams, P.T., 2014. Hydrogen production from biomass and plastic mixtures by pyrolysis-gasification. Int. J. Hydrogen Energy 39 (21), 10883–10891.
Artetxe, M., Lopez, G., Amutio, M., Barbarias, I., Arregi, A., Aguado, R., Bilbao, J., Olazar, M., 2015. Styrene recovery from polystyrene by flash pyrolysis in a conical spouted bed reactor. Waste Manag. 45, 126–133.
Asadullah, M., Zhang, S., Li, C.-Z., 2010. Evaluation of structural features of chars from pyrolysis of biomass of different particle sizes. Fuel Process. Technol. 91 (8), 877–881.
Bernardo, M.S., Lapa, N., Barbosa, R., Gonçalves, M., Mendes, B., Pinto, F., Gulyurtlu, I., 2009. Chemical and ecotoxicological characterization of solid residues produced during the co-pyrolysis of plastics and pine biomass. J. Hazard Mater. 166 (1), 309–317.
Bhattacharjee, N., Biswas, A.B., 2017. Pyrolysis of Alternanthera philoxeroides (alligator weed): effect of pyrolysis parameter on product yield and characterization of liquid product and bio char. J. Energy Inst. 91 (4), 605–618.
Chang, G., Miao, P., Wang, H., Wang, L., Hu, X., Guo, Q., 2018. A synergistic effect during the co-pyrolysis of Nannochloropsis sp. and palm kernel shell for aromatic hydrocarbon production. Energy Convers. Manag. 173, 545–554.
Chattopadhyay, J., Pathak, T., Srivastava, R., Singh, A., 2016. Catalytic co-pyrolysis of paper biomass and plastic mixtures (HDPE (high density polyethylene), PP (polypropylene) and PET (polyethylene terephthalate)) and product analysis. Energy 103, 513–521.
Chen, D., Chen, X., Sun, J., Zheng, Z., Fu, K., 2016a. Pyrolysis polygeneration of pine nut shell: quality of pyrolysis products and study on the preparation of activated carbon from biochar. Bioresour. Technol. 216, 629–636.
Chen, W., Shi, S., Zhang, J., Chen, M., Zhou, X., 2016b. Co-pyrolysis of waste newspaper with high-density polyethylene: synergistic effect and oil characterization. Energy Convers. Manag. 112, 41–48.
Chen, D., Zhou, J., Zhang, Q., Zhu, X., 2014. Evaluation methods and research progresses in bio-oil storage stability. Renew. Sustain. Energy Rev. 40, 69–79.
Chen, G., Andries, J., Luo, Z., Spliethoff, H., 2003. Biomass pyrolysis/gasification for product gas production: the overall investigation of parametric effects. Energy Convers. Manag. 44 (11), 1875–1884.
Chen, L., Wang, S., Meng, H., Wu, Z., Zhao, J., 2017. Synergistic effect on thermal behavior and char morphology analysis during co-pyrolysis of paulownia wood blended with different plastics waste. Appl. Therm. Eng. 111, 834–846.
Çepelioğullar, Ö., Pütün, A.E., 2014. Products characterization study of a slow pyrolysis of biomass-plastic mixtures in a fixed-bed reactor. J. Anal. Appl. Pyrolysis 110, 363–374.
Dewangan, A., Pradhan, D., Singh, R., 2016. Co-pyrolysis of sugarcane bagasse and low-density polyethylene: influence of plastic on pyrolysis product yield. Fuel 185, 508–516.
Diaz-Silvarrey, L.S., McMahon, A., Phan, A.N., 2018. Benzoic acid recovery via waste poly (ethylene terephthalate)(PET) catalytic pyrolysis using sulphated zirconia catalyst. J. Anal. Appl. Pyrolysis 134, 621–631.
Dimitrov, N., Krehula, L.K., Siročić, A.P., Hrnjak-Murgić, Z., 2013. Analysis of recycled PET bottles products by pyrolysis-gas chromatography. Polym. Degrad. Stabil. 98 (5), 972–979.
Dorado, C., Mullen, C.A., Boateng, A.A., 2015. Origin of carbon in aromatic and olefin products derived from HZSM-5 catalyzed co-pyrolysis of cellulose and plastics via isotopic labeling. Appl. Catal., B 162, 338–345.
Encinar, J., González, J., 2008. Pyrolysis of synthetic polymers and plastic wastes. Kinetic study. Fuel Process. Technol. 89 (7), 678–686.
Ephraim, A., Minh, D.P., Lebonnois, D., Peregrina, C., Sharrock, P., Nzihou, A., 2018. Co-pyrolysis of wood and plastics: influence of plastic type and content on product yield, gas composition and quality. Fuel 231, 110–117.
FAO, 2017. Statistics of Food and Agriculture Organisation of United Nations.
Gui, B., Qiao, Y., Wan, D., Liu, S., Han, Z., Yao, H., Xu, M., 2013. Nascent tar formation during polyvinylchloride (PVC) pyrolysis. Proc. Combust. Inst. 34 (2), 2321–2329.
Guo, X., Wang, S., Guo, Z., Liu, Q., Luo, Z., Cen, K., 2010. Pyrolysis characteristics of bio-oil fractions separated by molecular distillation. Appl. Energy 87 (9), 2892–2898.
Hasan, M.M., Wang, X.S., Mourant, D., Gunawan, R., Yu, C., Hu, X., Kadarwati, S., Gholizadeh, M., Wu, H., Li, B., 2017. Grinding pyrolysis of Mallee wood: effects of pyrolysis conditions on the yields of bio-oil and biochar. Fuel Process. Technol. 167, 215–220.
Herbert, G.J., Krishnan, A.U., 2016. Quantifying environmental performance of biomass energy. Renew. Sustain. Energy Rev. 59, 292–308.
Johansson, A.C., Sandström, L., Öhrman, O.G., Jilvero, H., 2018. Co-pyrolysis of woody biomass and plastic waste in both analytical and pilot scale. J. Anal. Appl. Pyrolysis 134, 102–113.
Jung, K.A., Woo, S.H., Lim, S.-R., Park, J.M., 2015. Pyrolytic production of phenolic compounds from the lignin residues of bioethanol processes. Chem. Eng. J. 259, 107–116.
Kajaste, R., 2014. Chemicals from biomass—managing greenhouse gas emissions in biorefinery production chains—a review. J. Clean. Prod. 75, 1–10.
Kelkar, S., Saffron, C.M., Andreassi, K., Li, Z., Murkute, A., Miller, D.J., Pinnavaia, T.J., Kriegel, R.M., 2015. A survey of catalysts for aromatics from fast pyrolysis of biomass. Appl. Catal., B 174, 85–95.
Kumagai, S., Fujita, K., Kameda, T., Yoshioka, T., 2016. Interactions of beech wood–polyethylene mixtures during co-pyrolysis. J. Anal. Appl. Pyrolysis 122, 531–540.
Lee, H.W., Kim, Y.-M., Jae, J., Jeon, J.-K., Jung, S.-C., Kim, S.C., Park, Y.-K., 2016. Production of aromatic hydrocarbons via catalytic co-pyrolysis of torrefied cellulose and polypropylene. Energy Convers. Manag. 129, 81–88.
Liu, J., Shimanoe, H., Nakabayashi, K., Miyawaki, J., Ko, S., Jeon, Y.-P., Yoon, S.-H., 2018. Preparation of isotropic pitch precursor for pitch-based carbon fiber through the co-carbonization of ethylene bottom oil and polyvinyl chloride. J. Ind. Eng. Chem. https://doi.org/10.1016/j.jiec.2018.06.039.
Liu, Z., Quek, A., Hoekman, S.K., Balasubramanian, R., 2013. Production of solid biochar fuel from waste biomass by hydrothermal carbonization. Fuel 103, 943–949.
Lu, P., Huang, Q., Bourtsalas, A.T., Chi, Y., Yan, J., 2018. Synergistic effects on char and oil produced by the co-pyrolysis of pine wood, polyethylene and polyvinyl chloride. Fuel 230, 359–367.
Lu, X., Jordan, B., Berge, N.D., 2012. Thermal conversion of municipal solid waste via hydrothermal carbonization: comparison of carbonization products to products from current waste management techniques. Waste Manag. 32 (7), 1353–1365.
Mafu, L.D., Neomagus, H.W., Everson, R.C., Strydom, C.A., Carrier, M., Okolo, G.N., Bunt, J.R., 2017. Chemical and structural characterization of char development during lignocellulosic biomass pyrolysis. Bioresour. Technol. 243, 941–948.
Mallick, D., Poddar, M.K., Mahanta, P., Moholkar, V.S., 2018. Discernment of synergism in pyrolysis of biomass blends using thermogravimetric analysis. Bioresour. Technol. 261, 294–305.
Mei, Y., Liu, R., 2017. Effect of temperature of ceramic hot vapor filter in a fluidized bed reactor on chemical composition and structure of bio-oil and reaction mechanism of pine sawdust fast pyrolysis. Fuel Process. Technol. 161, 204–219.
Melendi-Espina, S., Alvarez, R., Diez, M., Casal, M., 2015. Coal and plastic waste co-pyrolysis by thermal analysis–mass spectrometry. Fuel Process. Technol. 137, 351–358.
Nigam, P.S., Singh, A., 2011. Production of liquid biofuels from renewable resources. Prog. Energy Combust. Sci. 37 (1), 52–68.
Ning, S.-K., Hung, M.-C., Chang, Y.-H., Wan, H.-P., Lee, H.-T., Shih, R.-F., 2013. Benefit assessment of cost, energy, and environment for biomass pyrolysis oil. J. Clean. Prod. 59, 141–149.
Oyedun, A.O., Tee, C.Z., Hanson, S., Hui, C.W., 2014. Thermogravimetric analysis of the pyrolysis characteristics and kinetics of plastics and biomass blends. Fuel Process. Technol. 128, 471–481.
Paradela, F., Pinto, F., Gulyurtlu, I., Cabrita, I., Lapa, N., 2009. Study of the co-pyrolysis of biomass and plastic wastes. Clean Technol. Environ. 11 (1), 115–122.
Perkins, G., Bhaskar, T., Konarova, M., 2018. Process development status of fast pyrolysis technologies for the manufacture of renewable transport fuels from biomass. Renew. Sustain. Energy Rev. 90, 292–315.
Ro, D., Kim, Y.-M., Lee, I.-G., Jae, J., Jung, S.-C., Kim, S.C., Park, Y.-K., 2017. Bench scale catalytic fast pyrolysis of empty fruit bunches over low cost catalysts and HZSM-5 using a fixed bed reactor. J. Clean. Prod. 176, 298–303.
Sajdak, M., 2017. Impact of plastic blends on the product yield from co-pyrolysis of lignin-rich materials. J. Anal. Appl. Pyrolysis 124, 415–425.
Shadangi, K.P., Mohanty, K., 2015. Co-pyrolysis of Karanja and Niger seeds with waste polystyrene to produce liquid fuel. Fuel 153, 492–498.
Sharuddin, S.D.A., Abnisa, F., Daud, W.M.A.W., Aroua, M.K., 2016. A review on pyrolysis of plastic wastes. Energy Convers. Manag. 115, 308–326.
Shen, Y., Linville, J.L., Ignacio-de Leon, P.A.A., Schoene, R.P., Urgun-Demirtas, M., 2016. Towards a sustainable paradigm of waste-to-energy process: enhanced anaerobic digestion of sludge with woody biochar. J. Clean. Prod. 135, 1054–1064.
Sogancioglu, M., Yel, E., Ahmetli, G., 2017. Pyrolysis of waste high density polyethylene (HDPE) and low density polyethylene (LDPE) plastics and production of epoxy composites with their pyrolysis chars. J. Clean. Prod. 165, 369–381.
Solar, J., De Marco, I., Caballero, B., Lopez-Urionabarrenechea, A., Rodriguez, N., Agirre, I., Adrados, A., 2016. Influence of temperature and residence time in the pyrolysis of woody biomass waste in a continuous screw reactor. Biomass Bioenergy 95, 416–423.

Strezov, V., Evans, T.J., Hayman, C., 2008. Thermal conversion of elephant grass (Pennisetum Purpureum Schum) to bio-gas, bio-oil and charcoal. Bioresour. Technol. 99 (17), 8394–8399.
Sun, L., Zhang, X., Chen, L., Zhao, B., Yang, S., Xie, X., 2016. Comparision of catalytic fast pyrolysis of biomass to aromatic hydrocarbons over ZSM-5 and Fe/ZSM-5 catalysts. J. Anal. Appl. Pyrolysis 121, 342–346.
Suriapparao, D.V., Boruah, B., Raja, D., Vinu, R., 2018. Microwave assisted co-pyrolysis of biomasses with polypropylene and polystyrene for high quality bio-oil production. Fuel Process. Technol. 175, 64–75.
Taherzadeh, M.J., Karimi, K., 2008. Pretreatment of lignocellulosic wastes to improve ethanol and biogas production: a review. Int. J. Mol. Sci. 9 (9), 1621–1651.
Tang, Y., Huang, Q., Sun, K., Chi, Y., Yan, J., 2018. Co-pyrolysis characteristics and kinetic analysis of organic food waste and plastic. Bioresour. Technol. 249, 16–23.
Trubetskaya, A., Jensen, P.A., Jensen, A.D., Steibel, M., Spliethoff, H., Glarborg, P., 2015. Influence of fast pyrolysis conditions on yield and structural transformation of biomass chars. Fuel Process. Technol. 140, 205–214.
Van Putten, R.-J., van der Waal, J.C., De Jong, E., Rasrendra, C.B., Heeres, H.J., de Vries, J.G., 2013. Hydroxymethylfurfural, a versatile platform chemical made from renewable resources. Chem. Rev. 113 (3), 1499–1597.
Vyas, A., Chellappa, T., Goldfarb, J.L., 2017. Porosity development and reactivity changes of coal–biomass blends during co-pyrolysis at various temperatures. J. Anal. Appl. Pyrolysis 124, 79–88.
Wang, P., Jin, L., Liu, J., Zhu, S., Hu, H., 2013. Analysis of coal tar derived from pyrolysis at different atmospheres. Fuel 104, 14–21.
Wang, Q., Han, K., Gao, J., Li, H., Lu, C., 2017. The pyrolysis of biomass briquettes: effect of pyrolysis temperature and phosphorus additives on the quality and combustion of bio-char briquettes. Fuel 199, 488–496.
Xu, Y., Zeng, X., Luo, G., Zhang, B., Xu, P., Xu, M., Yao, H., 2016. Chlorine-Char composite synthesized by co-pyrolysis of biomass wastes and polyvinyl chloride for elemental mercury removal. Fuel 183, 73–79.
Yu, J., Sun, L., Ma, C., Qiao, Y., Yao, H., 2016. Thermal degradation of PVC: a review. Waste Manag. 48, 300–314.
Zhang, B., Zhong, Z., Zhang, J., Ruan, R., 2018. Catalytic fast co-pyrolysis of biomass and fusel alcohol to enhance aromatic hydrocarbon production over ZSM-5 catalyst in a fluidized bed reactor. J. Anal. Appl. Pyrolysis 133, 147–153.
Zhao, B., O'Connor, D., Zhang, J., Peng, T., Shen, Z., Tsang, D.C., Hou, D., 2018a. Effect of pyrolysis temperature, heating rate, and residence time on rapeseed stem derived biochar. J. Clean. Prod. 174, 977–987.
Zhao, Y., Wang, Y., Duan, D., Ruan, R., Fan, L., Zhou, Y., Dai, L., Lv, J., Liu, Y., 2018b. Fast microwave-assisted ex-catalytic co-pyrolysis of bamboo and polypropylene for bio-oil production. Bioresour. Technol. 249, 69–75.
Zheng, Y., Tao, L., Yang, X., Huang, Y., Liu, C., Zheng, Z., 2018. Insights into pyrolysis and catalytic co-pyrolysis upgrading of biomass and waste rubber seed oil to promote the formation of aromatics hydrocarbon. Int. J. Hydrogen Energy 43 (34), 16479–16496.
Zhou, H., Wu, C., Onwudili, J.A., Meng, A., Zhang, Y., Williams, P.T., 2015. Polycyclic aromatic hydrocarbons (PAH) formation from the pyrolysis of different municipal solid waste fractions. Waste Manag. 36, 136–146.